

## Composite Resins Based on Novel and Highly Reactive Bisglycidyl Methacrylate Monomers

Ana María Herrera-González, Norma Beatriz D'Accorso, Carlos Enrique Cuevas-Suárez, Mirta Liliana Fascio, Jesús García-Serrano, Miriam Martins Alho, Juan Eliezer Zamarripa-Calderón

Universidad Autónoma del Estado de Hidalgo - Instituto de Ciencias Básicas e Ingeniería, Carretera Pachuca-Tulancingo Km. 4.5 Colonia Carboneras, Mineral de la Reforma, Hidalgo, 42183, México

Correspondence to: A. M. Herrera-González (E-mail: mherrera@uaeh.edu.mx)

**ABSTRACT:** Three new bisglycidyl monomers; 1,4-bis((2-hydroxy-3-methacryloxypropoxy) methyl)benzene (MB-Phe-OH), 1,4-bis(2-hydroxy-3-methacryloxypropoxy)2-cis-butene (MB-Cis-OH), and 1,7-bis(2-hydroxy-3-methacryloxypropoxy)heptane (MB-1,7-OH); were synthesized and used as Bis-GMA/TEGDMA (bisphenolglycidyl methacrylate/triethylene glycol dimethacrylate) composite resin additives. Flexural properties and double bond conversion of the dental resins composed of silanized inorganic filler and organic matrices containing new monomers were evaluated. The composite resins formulated, using the monomers MB-Cis-OH and MB-1,7-OH, have mechanical properties and double bond conversion comparable with those of Bis-GMA/TEGDMA composite resin used as control. The composite containing the new monomer MB-Phe-OH has better flexural properties (flexural strength 65.01 MPa and flexural modulus 5675.91 MPa) than the control composite resin (flexural strength 52.85 MPa and flexural modulus 4879.72 MPa); this could be attributed to the molecular structure of the monomer and its high double bond conversion level of 74.19%. The new bisglycidyl methacrylate monomer MB-Phe-OH could be potentially useful in the development of new organic matrices for dental composite resins with high double bond conversion and enhanced mechanical properties. © 2014 Wiley Periodicals, Inc. *J. Appl. Polym. Sci.* 2014, 131, 40971.

**KEYWORDS:** biomaterials; composites; crosslinking; photopolymerization; resins

Received 14 January 2014; accepted 4 May 2014

DOI: 10.1002/app.40971

### INTRODUCTION

Polymerization of multifunctional monomers like bisglycidyl methacrylates produces highly crosslinked polymers which can find many applications in dentistry such as dental composites, dental adhesives, bonding agents and cements, and fissure sealants.<sup>1,2</sup> Dental composite resins consist of a blend of hard inorganic particles bound to a soft organic matrix with a silane coupling agent. The organic matrix comprises a monomer system and an initiator system for free radical polymerization. Light-curable bisglycidyl methacrylate monomers, such as Bis-GMA and TEGDMA are the most commonly used monomers in commercial dental materials. The inorganic filler consists of nanosized particulates (glass, quartz, and/or fused silica) and a coupling agent, usually an organo-silane, which chemically bonds the filler to the organic matrix.<sup>3–7</sup> Incorporation of inorganic filler helps to enhance the mechanical and thermal properties of the composite materials. The composite can be prepared by addition of inorganic filler or in situ sol-gel reactions of dual curable monomers.<sup>8–10</sup> Since dental composite resins were invented, the most important changes have involved

improving the filler and the mechanism of initiation, which has been developed to produce materials that are more easily handled and demonstrate better clinical performance.<sup>3</sup> Despite this, some drawbacks like insufficient wear resistance and bulk fracture are some of the major reasons for replacing these dental restorations.<sup>11–17</sup> In a contemporary dental composite resin restorative system, a large number of methacrylate groups in the cross-linked polymer are left unreacted which could lead to the decrease of its physical, mechanical, and chemical properties.<sup>18–21</sup>

To solve these issues and improve the performance of this kind of materials, plenty of research is being made. Main topics include synthesis of new monomers with high strength and higher double bond conversion that could lead to improved mechanical properties of the restorative materials. Other topics include new monomers system with less polymerization shrinkage, less water sorption, and water solubility, as well as monomers with anticariogenic and antimicrobial activity.<sup>6,17</sup> In this study, new bisglycidyl methacrylate monomers were synthesized and used as a component for dental restoration material. The

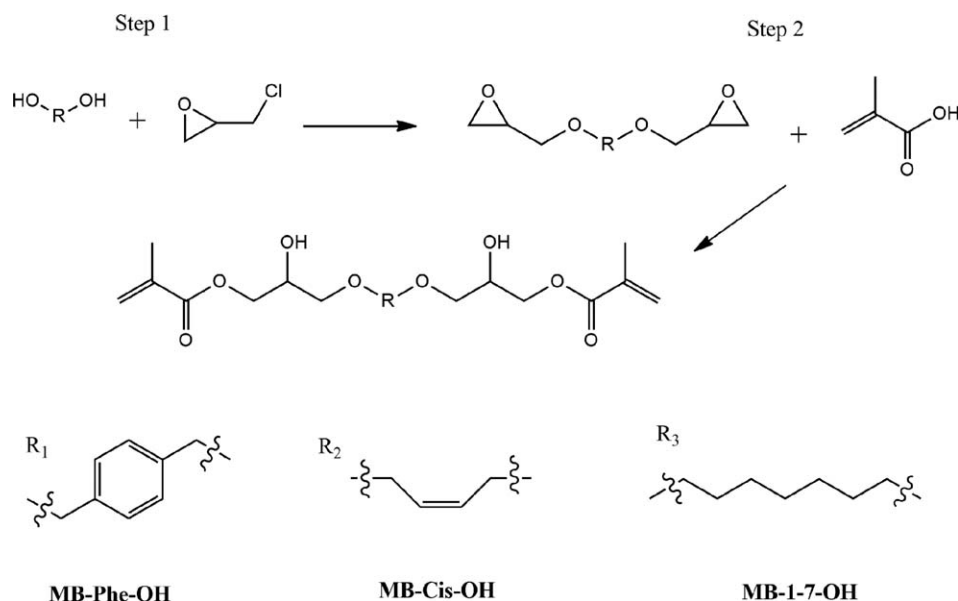


Figure 1. General synthetic route of the bisglycidyl methacrylates monomers.

goal of this work is to investigate the material properties of dental resins containing novel bisglycidyl methacrylate monomers as reactive components of Bis-GMA/TEGDMA.

## EXPERIMENTAL

### Materials and Instruments

All materials and solvents used for the synthesis of monomers, silanization of nanoparticles, and preparation of nanocomposites are commercially available from Sigma-Aldrich and were used as received.

NMR spectra were recorded on a Jeol Eclipse +400 spectrometer. FTIR spectra were obtained on a Perkin Elmer FTIR System 2000. The elemental analysis was recorded with a Perkin Elmer analyzer (2499 C, H, N, Serie II). Photopolymerization was made using a Bluephase® 16i dental photocuring unit using a light intensity of 1000 mW/cm<sup>2</sup> (irradiation wavelength 430–490 nm). Flexural properties were measured with an Instron 4465 universal testing machine. Details of all procedures will be given thereafter.

### Synthesis of Bisglycidyl Methacrylates Monomers

Synthesis of bisglycidyl methacrylates monomers were carried out in two-step reactions (Figure 1). The general procedure is described for the MB-Phe-OH monomer. Synthesis of MB-Cis-OH and MB-1,7-OH were made under the same conditions.

#### Step 1. General Procedures for the Synthesis of Bisglycidyl Ether

The reaction was carried out in a two-necked round bottomed flask equipped with a magnetic stir bar and purged with dry argon gas. The reagents used at the ratio of 1 : 2.5 mole of diol to epichlorohydrin and 2 mol of sodium hydride were stirred with 15 mL of DMF. Then, the system was immersed in a water bath maintained at 50°C under vigorous stirring for 18 h. The reaction mixture was extracted three times with water and ethyl ether. The organic layer was then dried over Na<sub>2</sub>SO<sub>4</sub> and the solvent was evaporated under vacuum. The product was

purified by column chromatography (aluminum oxide) using cyclohexane/acetone (90 : 10) as eluent.

Intermediate glycidyl ether compounds were identified using <sup>1</sup>HNMR, FTIR, and elemental analysis. Glycidylether 1,4-bis((oxiran-2-ylmethoxy)methyl)benzene (BE-Phe-OH). <sup>1</sup>HNMR (DCCl<sub>3</sub>, 400 MHz) δ (ppm): 7.34 (aromatic protons), 3.19 (—CH— epoxy), 2.81 (—CH<sub>2</sub>— epoxy), 2.62 (—CH<sub>2</sub>— epoxy). FTIR (KBr, cm<sup>-1</sup>): 1364 (ν<sub>asym</sub>C—O—C), 914 (ν<sub>sym</sub>C—O—C), 751 (epoxy). Elemental Analysis: C<sub>14</sub>H<sub>18</sub>O<sub>4</sub> (calculated) found: %C (67.18) 67.21, %H (7.25) 7.01, %O (25.57) 25.78. Glycidylether cis-1,4-bis(oxiran-2-ylmethoxy)2-butene (BE-Cis-OH); <sup>1</sup>HNMR (DCCl<sub>3</sub>, 400 MHz) δ (ppm): 3.16 (—CH— epoxy), 2.81 (—CH<sub>2</sub>— epoxy), 2.61 (—CH<sub>2</sub>— epoxy). FTIR (KBr, cm<sup>-1</sup>): 1095 (ν<sub>sym</sub>C—O—C), 1011 (ν<sub>sym</sub>C—O—C), 761 (epoxy group). Elemental Analysis: C<sub>10</sub>H<sub>16</sub>O<sub>4</sub> (calculated) found: %C (59.98) 59.62, %H (8.05) 8.02, %O (31.97) 32.36. Glycidylether 1,7-bis(oxiran-2-ylmethoxy)heptane (BE-1,7-OH); <sup>1</sup>HNMR (DCCl<sub>3</sub>, 400 MHz) δ (ppm): 3.14 (—CH— epoxy), 2.79 (—CH<sub>2</sub>— epoxy), 2.61 (—CH<sub>2</sub>— epoxy). FTIR (KBr, cm<sup>-1</sup>): 1095 (ν<sub>sym</sub>C—O—C), 1011 (ν<sub>sym</sub>C—O—C), 761 (epoxy). Elemental Analysis: C<sub>13</sub>H<sub>24</sub>O<sub>4</sub> (calculated) found: %C (63.91) 63.71, %H (9.90) 9.84, %O (26.19) 26.45.

#### Step 2. General Procedures for the Synthesis of Bisglycidyl Methacrylates Monomers

The synthesis was carried out in a two-necked round bottom flask, fitted with a magnetic stirrer, purged with dry argon gas, sealed, and covered from the light. Bisglycidyl ether obtained in step 1 was added to a solution of methacrylic acid in triethylamine (0.2 wt %) in a molar ratio 1 : 3. Hydroquinone (0.2 wt %) was used as free radical polymerization inhibitor. The system was immersed in a water bath maintained at 60°C during 24 h under vigorous stirring. After completion of the reaction, 40 mL of ethyl acetate was added into the reaction vessel. Several extractions with HCl (2M) and saturated NaHCO<sub>3</sub> solution were made. The organic layer was separated and evaporated under vacuum.

Final products were identified using  $^1\text{H}$ NMR, FTIR, and elemental analysis. MB-Phe-OH (yield: 51.45 %).  $^1\text{H}$ NMR ( $\text{DCCl}_3$ , 400 MHz)  $\delta$  (ppm): 7.24 (aromatic protons), 6.04 and 5.52 ( $\text{CH}_2=\text{C}$ ), 4.01 (O—H). FTIR (KBr,  $\text{cm}^{-1}$ ): 3464 ( $\nu\text{O—H}$ ), 2865 ( $\nu_{\text{asym}}\text{C—H}$ ), 1716 ( $\nu\text{C=O}$ ), 1636 ( $\nu\text{C=C}$ ), 1455 ( $\nu\text{—CH}_2\text{—}$ ), 813 ( $\nu\text{C=C}$ ). Elemental Analysis:  $\text{C}_{22}\text{H}_{30}\text{O}_8$  (calculated) found: %C (62.55) 62.44, %H (7.16) 7.47, %O (30.30) 30.40. MB-Cis-OH (yield: 56.5%).  $^1\text{H}$ NMR ( $\text{DCCl}_3$ , 400 MHz)  $\delta$  (ppm): 6.14 and 5.60 ( $\text{CH}_2=\text{C}$ ), 5.75 ( $\text{—CH}_2\text{=CH}_2\text{—}$ ), 3.68 (O—H). FTIR (KBr,  $\text{cm}^{-1}$ ): 3441 ( $\nu\text{O—H}$ ), 2928 ( $\nu_{\text{asym}}\text{C—H}$ ), 1718 ( $\nu\text{C=O}$ ), 1637 ( $\nu\text{C=C}$ ). Elemental Analysis:  $\text{C}_{18}\text{H}_{28}\text{O}_8$  (calculated) found: %C (58.05) 58.00, %H (7.58) 7.67, %O (34.37) 34.33. MB-1,7-OH (yield: 62.25 %).  $^1\text{H}$ NMR ( $\text{DCCl}_3$ , 400 MHz)  $\delta$  (ppm): 6.14 and 5.59 ( $\text{CH}_2=\text{C}$ ), 3.87 (O—H), 1.96 ( $\text{—CH}_3\text{—}$ ). FTIR (KBr,  $\text{cm}^{-1}$ ): 3458 ( $\nu\text{OH}$ ), 2858 ( $\nu_{\text{asym}}\text{C—H}$ ), 1711 ( $\nu\text{C=O}$ ), 1634 ( $\nu\text{C=C}$ ). Elemental Analysis:  $\text{C}_{21}\text{H}_{30}\text{O}_8$  (calculated) found: %C (60.56) 60.52, %H (8.71) 8.64, %O (30.73) 30.84.

### Bulk Polymerization of Bisglycidyl Methacrylate Monomers Under Visible Light Irradiation

MB-Cis-OH, MB-Phe-OH, or MB,1,7-OH monomers were cross-linked in a quiescent photopolymerization. Camphorquinone (CQ) and Ethyl-4-(dimethylamino)benzoate (E4DMAB) were used as the photoinitiator system (1 wt % each). The experiments were carried out at room temperature under atmospheric conditions. The polymerizable composition (monomer + photoinitiator) was prepared in Pyrex test tubes and then irradiated for 5, 10, 20, and 40 s using a Bluephase 16i® dental photocuring unit equipped with a LED light source. All mixtures were prepared and used immediately.

### Polymer Gel Fraction Percent Measurements

Gel percentage for each sample was measured by sol-gel extractions. Once the sample was polymerized, it was weighted, triturated, and placed on a 10 mL Erlenmeyer flask containing 5 mL of acetone and equipped with a magnetic stirrer. After 6 h under vigorous stirring, the acetone was filtered off. Then another 5 mL of acetone were added. This cycle was repeated three times. After the last cycle, the sample was dried for 12 h and weighted again. The gel percentage was then calculated as

$$\% \text{ gel content} = \left[ \frac{W_f}{W_i} \right] \times 100$$

where  $W_f$  is the weight of the sample after the acetone washing and  $W_i$  is the weight of the sample before the acetone washing.

### Silanization of Silica Nanoparticles

Silica nanoparticles were silanized with 3-(trimethoxysilyl)propyl methacrylate (MPS) following the Chen and Brauer method.<sup>22</sup> The amount of silane in grams to obtain a minimum coverage of the silica nanoparticles is given by the following equation<sup>23</sup>:

$$X = \left( \frac{A}{\omega} \right) f$$

where  $(A)$  is the surface area of the silica nanoparticles ( $200 \text{ m}^2/\text{g}$ ),  $(\omega)$  is the surface coverage per gram of silane MPS ( $2525 \text{ m}^2/\text{g}$ ), and  $(f)$  is the amount of silica in grams.

**Table I.** Organic Matrix Compositions of the Composites Evaluated

Material	Monomer 1 (wt %)	Monomer 2 (wt %)	Monomer 3 (wt %)
M1	Bis-GMA (65)	TEGDMA (35)	
M2	Bis-GMA (65)	TEGDMA (20)	MB-Phe-OH (15)
M3	Bis-GMA (65)	TEGDMA (20)	MB-Cis-OH (15)
M4	Bis-GMA (65)	TEGDMA (20)	MB-1,7-OH (15)

To a one-necked round bottom flask equipped with a magnetic stir bar, silica (5 g), MPS (0.44 g), cyclohexane (100 mL), and *n*-propylamine (0.1 g) were added and stirred at room temperature for 30 min and then at  $60^\circ\text{C}$  for another 30 min. The reaction vessel was then placed in a rotary evaporator. After solvent elimination, the resulting powder was dried at  $60^\circ\text{C}$  in a vacuum oven for 24 h. Silanization of silica nanoparticles were identified by FTIR and TEM. FTIR (KBr,  $\text{cm}^{-1}$ ): 2945 ( $\nu_{\text{asym}}\text{H—C—H}$ ), 2943 ( $\nu_{\text{sym}}\text{H—C—H}$ ), 1702 ( $\nu\text{C=O}$ ), 1638 ( $\nu\text{C=C}$ ), 1111 ( $\nu\text{Si—O—Si}$ ), 815 ( $\delta_{\text{sym}}\text{Si—O—Si}$ ), 472 ( $\delta_{\text{sym}}\text{Si—O—Si}$ ).

### Preparation of Composites

The resin matrix consisted of 65 wt % BisGMA, 20 wt % TEGDMA, 15 wt % of the new monomer, (MB-1,7-OH, MB-Cis-OH, or MB-Phe-OH), and 1 wt % of the photoinitiator system CQ/E4DMAB. BisGMA/TEGDMA composite, in a mass ratio of 65 wt %, and 35 wt % was used as the control. To a one-necked round bottom flask equipped with a magnetic stirrer a mixture of the resin matrix components was dispersed into 90% ethanol (mass fraction) followed by vigorous stirring for 2 h. The ethanol was removed by vacuum evaporation, and then the silanized silica (40 wt %) was mixed with the resin matrix by hand spatulation. Table I summarizes the organic matrix compositions.

### Measurement of Double Bond Conversion

The double bond conversion of the composites formulation was determined by infrared spectroscopy. Totally, 15 mg of the composite were thoroughly mixed with 150 mg of bromide potassium salt. This mixture was placed into a pelleting device and then compressed in a press to obtain a pellet of about 0.5 mm in thickness. The pellet was then placed into a standard sample holder. FTIR spectra of both uncured and cured samples were obtained in the absorbance region of over  $4000\text{--}300 \text{ cm}^{-1}$  with a resolution of  $4 \text{ cm}^{-1}$  and a total of 32 scans per spectrum. For each spectrum, the height of aliphatic  $\text{C=C}$  ( $A_{1638}$ ) peak absorption at  $1638 \text{ cm}^{-1}$  and the aromatic  $\text{C=C}$  ( $A_{1609}$ ) peak absorption at  $1609 \text{ cm}^{-1}$  was determined. Aromatic  $\text{C=C}$  vibration was used as an internal reference. The double bond conversion was determined according to the following equation:

$$\text{Double bond conversion (\%)} = 100 \left[ 1 - \frac{\left( \frac{A_{1638}}{A_{1609}} \right)_{\text{polymer}}}{\left( \frac{A_{1638}}{A_{1609}} \right)_{\text{monomer}}} \right]$$

### Flexural Properties

Flexural strength was measured in accordance with the International Standard Organization (ISO) Specification No. 4049, while elastic modulus was measured in accordance to the American National Standard Institute/American Dental Association

(ANSI/ADA) Specification No. 27. Bar-specimens were prepared by filling the uncured samples into a stainless steel mold (25 mm × 2 mm × 2 mm). The samples were irradiated on both sides by the overlapping technique using the Bluephase 16i® dental photocuring unit. Each overlap was light-cured for 15 s using the soft cure mode (400 mW/cm<sup>2</sup>). Five specimen bars were prepared and stored in distilled water at 37 ± 1°C in a dark environment for 24 h. A three-point bending test was carried out to evaluate the flexural properties of the cured samples with an Instron 4465 universal testing machine at a cross-head speed of 1.00 mm/min until fracture occurred. The flexural strength ( $\sigma$ ) and flexural modulus ( $E$ ), both in MPa were calculated using the following equations:

$$\sigma = \frac{3Fl}{2bh^2} \quad E = \frac{F_1 l^3}{4bh^3 d}$$

here  $F_1$  represents the load in Newton exerted on the specimen,  $F$  is the maximum load in Newton exerted on the specimen at the point fracture,  $l$  is the distance in mm between the supports,  $h$  is the height of specimen in mm measured immediately prior to testing,  $b$  is the width of specimen in mm measured immediately prior to testing, and  $d$  is the deflection corresponding to the load  $F_1$ .

### Statistical Analysis

Double bond conversion, flexural strength and flexural modulus results were analyzed using one-way analysis of variance ANOVA and Tukey's post-hoc tests for multiple comparisons. Statistical differences were considered if  $P < 0.05$ .

## RESULTS AND DISCUSSION

### Syntheses of the Bisglycidyl Methacrylates Monomers

The general synthetic route and the chemical structures for the bisglycidyl methacrylates monomers are depicted in Figure 1. They have been fully confirmed by <sup>1</sup>HNMR and FTIR spectroscopy as well as elemental analysis.

Monomers MB-Phe-OH, MB-Cis-OH, and MB-1,7-OH were the main product in the reaction. These were synthesized by esterification via epoxy ring-opening addition of the intermediate compound with methacrylic acid. This reaction was performed using an excess of methacrylic acid so that it could further react with all -OH groups to form the esterification product. The three new monomers were obtained with good yields between 51 and 62%.<sup>24</sup> Some other authors have reported similar yields for the synthesis of new bisglycidyl methacrylates.<sup>25–29</sup>

FTIR spectra of these new compounds revealed that the absorption band at 910 cm<sup>-1</sup>, corresponding to the epoxy group of the intermediate compound disappears, and new absorption bands at 3471 cm<sup>-1</sup> ( $\nu$ O-H), 1697 cm<sup>-1</sup> ( $\nu$ C=O), 1638 cm<sup>-1</sup> ( $\nu$ C=C) and absorption band at 811 cm<sup>-1</sup> ( $\delta$ C=C) appear. Figure 2 shows spectra of monomers corresponding to <sup>1</sup>HNMR. In these spectra, distinctive signals assigned to -C=C-H *cis* (6.1 ppm), C=C-H *trans* (5.5–5.57 ppm), and -CH<sub>3</sub> (1.9 ppm) were observed in the three novel monomers, while the two signals between 3.3–3.4 ppm and 2.7–2.9 ppm corresponding to the epoxide -CH and -CH<sub>2</sub> groups of the starting material disappeared. This suggests that the epoxy groups reacted

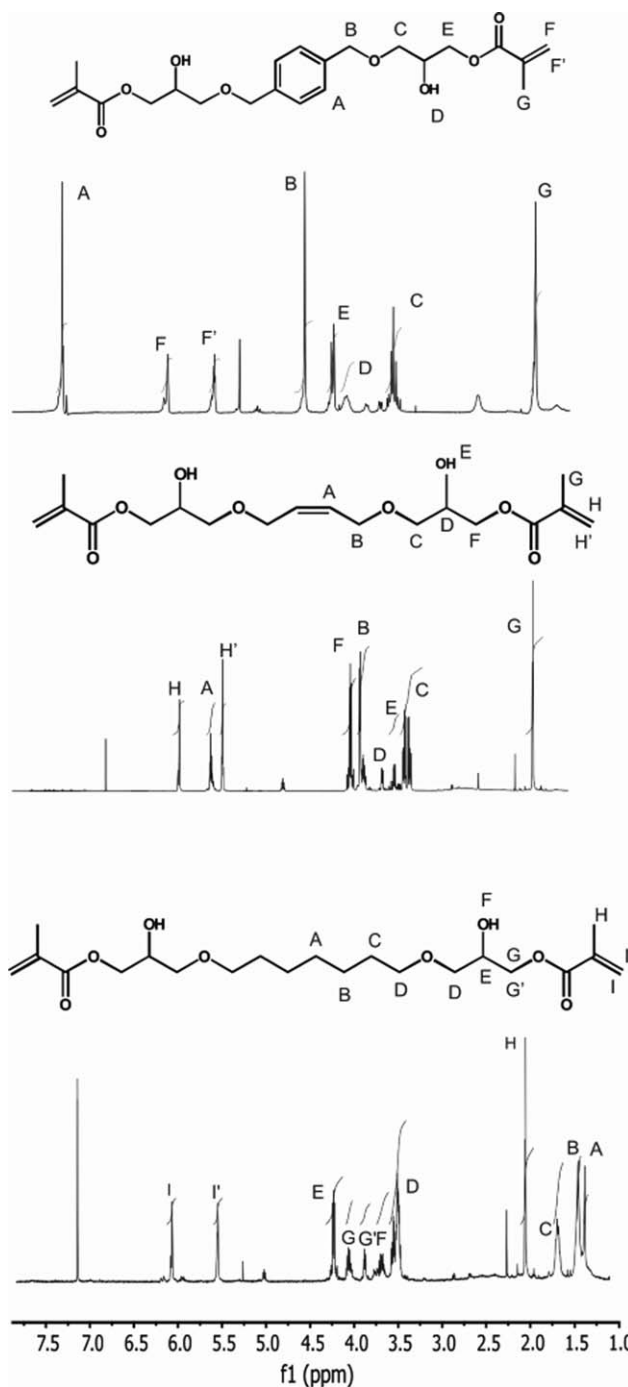


**Figure 2.** <sup>1</sup>HNMR Spectra of MB-Phe-OH, MB-Cis-OH and MB-1,7-OH monomers. [Color figure can be viewed in the online issue, which is available at [wileyonlinelibrary.com](http://wileyonlinelibrary.com).]

completely with methacrylic acid and that methacrylate groups were introduced successfully. Elemental analysis confirmed the formation of the new monomers (see Experimental).

### Bulk Polymerization of Bisglycidyl Methacrylate Monomers Under Visible Light Irradiation

MB-Phe-OH, MB-Cis-OH, or MB-1,7-OH monomers were irradiated under atmospheric conditions in quiescent polymerization. Once the monomers were exposed to the visible light



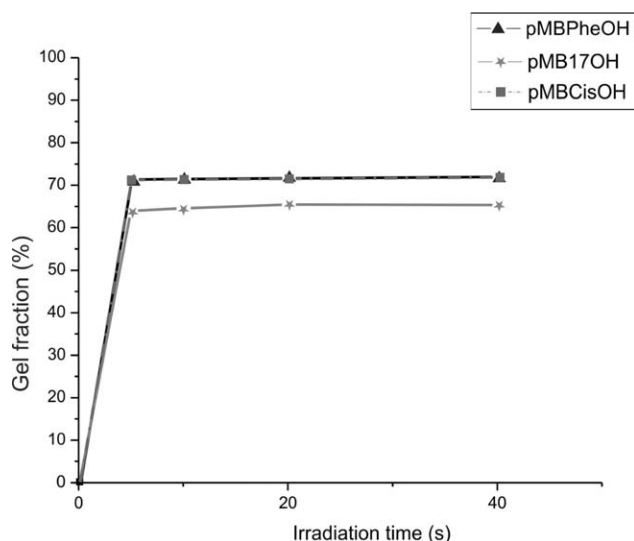


**Figure 3.** Variation of gel fraction percent (%), versus the irradiation time of the monomers.

irradiation, they polymerized readily. Atmospheric oxygen did not inhibit their polymerization because the three new monomers are highly reactive due to their tetra functionality. The monomer intrinsic reactivity increases with the number of terminal acrylic groups in the monomer structure.

The polymerization time increases the gel fraction percent, as expected. Gel fraction percent as a function of irradiation time was obtained after the reaction polymerization by sol-gel extractions. Figure 3 shows the gel fraction percent (%) versus the irradiation time for the monomers studied.

Crosslinking results of the occurrence of gelation at some time in the polymerization. At this point, the formation of a gel fraction or insoluble polymer fraction is observed. This gel fraction is insoluble in all solvents at elevated temperatures under conditions where polymer degradation does not occur.<sup>30</sup> In Figure 3, It is clearly observed that when the monomers were irradiated with visible light, crosslinking polymerization was very fast and reached a gel fraction conversion rates of above 65% in a very short period of time. However, 5 s after that, there were no changes in the gel fraction conversion percentage with the increase of irradiation time. Complete gel fraction conversion almost never occurs because the polymer immobilization, vitrification, gelation, or steric isolation inhibits the polymerization reaction. This behavior has been observed in some multifunctional glycidyl methacrylates.<sup>31–33</sup>

Figure 4 shows the FTIR spectra of MB-Cis-OH monomer and homopolymer. FTIR spectrum of the monomer (bottom) shows a band at  $1638\text{ cm}^{-1}$  corresponding to the stretching vibration of the  $\text{C}=\text{C}$  ( $\nu$ ) methylene terminal group, while in the FTIR spectrum of the polymer spectrum (top), this absorption band has been reduced drastically due to polymerization reaction. Once the sol-gel extractions procedures have been done, the non-gel portion of the polymer, referred as sol, was eliminated. It is important to note that the band at  $1638\text{ cm}^{-1}$ , which corresponds to the stretching vibration of the  $\nu\text{C}=\text{C}$  methylene terminal group, did not disappear at all after the sol-gel extraction. The

presence of this band in the gel fraction corresponds to those double bonds trapped into the polymer network. When crosslinking of monomers with functionality greater than two (like MB-Phe-OH, MB-Cis-OH, and MB-1,7-OH) occurs, molecules may react at one end only and some double bonds could remain unreacted due to polymer immobilization.

#### Preparation of Nanocomposites

Table I shows the composition of the organic matrix for the dental composites evaluated in this study. The mass ratio of the new monomers was maintained constant to evaluate their effect on selected mechanical properties. Also, inorganic filler content was maintained constant for all the composites.

The inorganic filler of dental composite evaluated in this study contains silanized silica nanoparticles. The silanization mechanism of the silica nanoparticles was previously described.<sup>34,35</sup> In this mechanism, the molecules of silane are chemically bonded to the surface of silica nanoparticles by siloxane ( $\text{Si}-\text{O}-\text{Si}$ ). For composite resin preparation, a silane coupling agent is used to improve adhesion between the inorganic filler and the resin matrix into a composite and to significantly reduce the presence of air between the interfaces which could impair the material.<sup>36,37</sup> It is well known that dental composites which contain silanized filler exhibit superior mechanical properties and wear resistance as well as less water sorption and lower water solubility than those that do not.<sup>38</sup>

The maximum amount of silica nanoparticles admitted by the organic matrix was 40 wt %. The addition of a larger amount of silica nanoparticles increases the viscosity of the composite

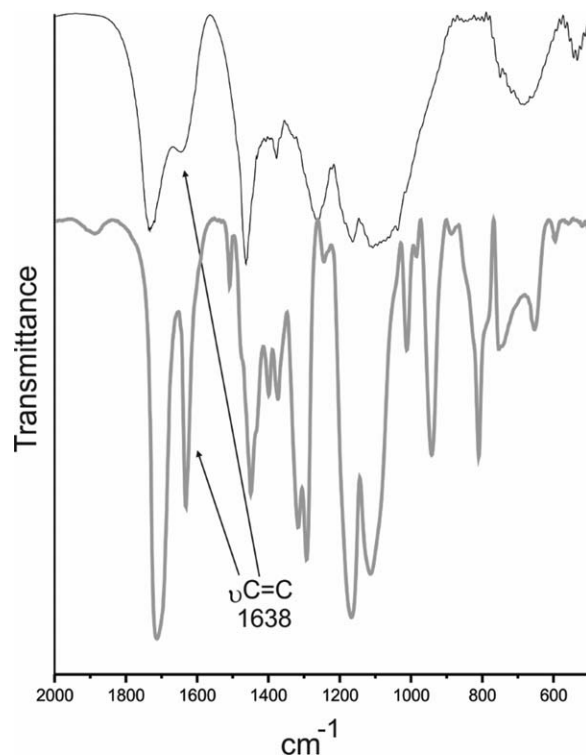


**Figure 4.** FTIR spectra of MB-Cis-OH (bottom) and poly(MB-Cis-OH) (top).

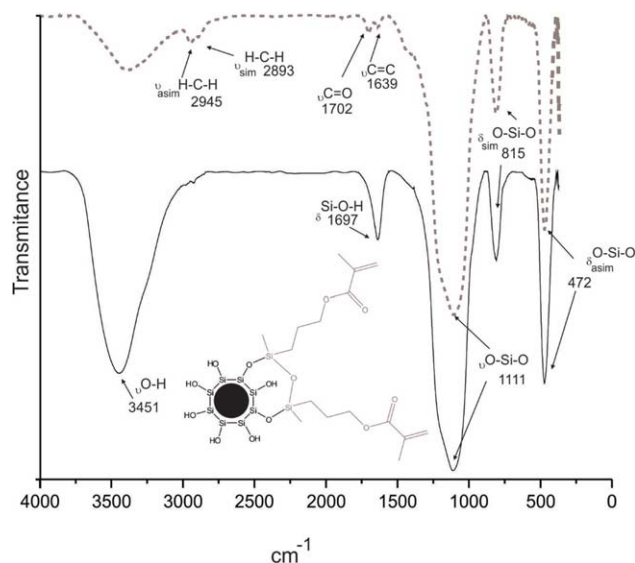


**Figure 5.** FTIR spectra of the silica nanoparticles before (down) and after (up) silanization. [Color figure can be viewed in the online issue, which is available at [wileyonlinelibrary.com](http://wileyonlinelibrary.com).]

resin beyond the odontologic handling capabilities. Besides the viscosity of the organic matrix evaluated, it is important to note that in this study, a nanometric sized inorganic filler (0,2-0,3  $\mu\text{m}$ ) with a high specific surface area (200  $\text{m}^2/\text{g}$ ) was used. This implies that the percentage of MPS coupling agent required for complete and uniform coverage of silica surface increases, and therefore the filler content decreases.<sup>39</sup>

Figure 5 shows the FTIR spectrum before and after the silanization process of silica nanoparticles. The FTIR spectrum of silica nanoparticles before silanization procedure showed the following absorption bands: a broad band at 3451  $\text{cm}^{-1}$  due to the presence of surface hydroxyl groups stretching vibration ( $\nu\text{O-H}$ ); at 1697  $\text{cm}^{-1}$ , the band due to hydroxyl group bending vibration ( $\delta\text{Si-O-H}$ ); the signal at 1111  $\text{cm}^{-1}$  which is attributed to the siloxane stretching vibration ( $\nu\text{O-Si-O}$ ); and the bands at 815 and 472  $\text{cm}^{-1}$  due to siloxane scissoring and rocking vibration ( $\delta_{\text{sym}}$  and  $\delta_{\text{asym}}$  O-Si-O). The FTIR spectrum of silica nanoparticles treated with MPS showed the bands: at 2945 and 2943  $\text{cm}^{-1}$  due to methylene asymmetrical and symmetrical stretching ( $\nu_{\text{asym}}$  and  $\nu_{\text{sym}}$  H-C-H); at 1702  $\text{cm}^{-1}$  due to free carbonyl stretching vibration ( $\nu\text{C=O}$ ); and at 1638  $\text{cm}^{-1}$  due to stretching vibration of the  $\nu\text{C=C}$  in the silane coupling agent. Absorption bands at 1111, 815, and 472  $\text{cm}^{-1}$  due to stretching ( $\nu$ ), scissoring ( $\delta_{\text{sym}}$ ) and rocking ( $\delta_{\text{asym}}$ ) of siloxane bonds still persist. This is understood by the fact that these bonds result unaffected by the silanization process.

The silanization process was also confirmed by TEM analysis. Figure 6 shows the TEM images before (left) and after (right) the silanization process. The TEM image before the silanization shows that silica nanoparticles are roughly spherical and highly uniform in size and the morphology is homogenous. We can also note that silica nanoparticles are forming several stringy-shape clusters. This occurs because of its high specific surface

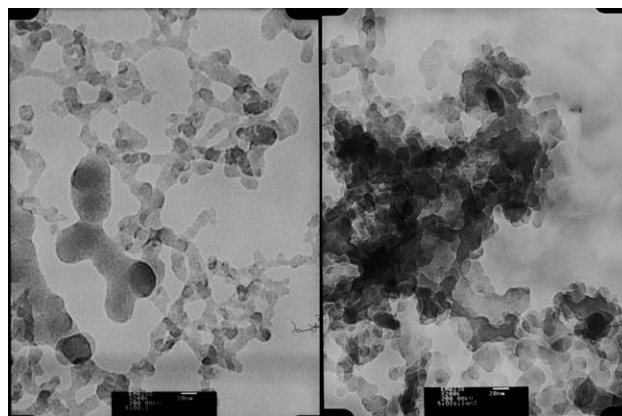


**Figure 6.** TEM images of silica nanoparticles before (left) and after (right) silanization.

area (200  $\text{m}^2/\text{g}$ ) which leads itself to readily form aggregates by hydrogen bond interactions in silica surface. The TEM image after the silanization process shows that the morphology and size of silica nanoparticles are not affected. Nevertheless, once the silane coupling agent is attached to the silica surface, the morphology and size of the clusters change. Silica clusters are heterogeneous and bigger due the formation of covalent bonds between the silica nanoparticles and the silane coupling agent.

#### Measurement of Double Bond Conversion

The average values of double bond conversion, flexural strength, and flexural modulus for the tested composite materials with standard deviations (SD) are summarized in Table II. Comparing the results of the double bond conversion, it can be seen that the composite that contains MB-Phe-OH statistically exhibits significantly higher double bond conversion than BisGMA/TEGDMA used as the control, whereas the composite which contains MB-Cis-OH and MB-1,7-OH did not show any significant differences compared to the control.

The double bond conversion of a resin depends on the chemical structure of the bisglycidyl methacrylate monomer and some polymerization conditions like atmosphere, temperature, light intensity, and photoinitiator concentration.<sup>40</sup> In this study, the composite formulated with the new MB-Phe-OH monomer exhibited a significantly higher double bond conversion. This behavior could be because the monomer MB-Phe-OH has the highest molecular weight compared to the other two

**Table II.** Flexural Properties and Degree of Conversion of the Dental Composite Evaluated [Mean(S.D.)],  $n = 5$

Material	Flexural strength (MPa)	Flexural modulus (MPa)	Degree of conversion (%)
M1	52.85 (3.9) <sup>b</sup>	4879.72 (219.45) <sup>b</sup>	70.27 (0.12) <sup>b</sup>
M2	65.01 (5.2) <sup>a</sup>	5675.91 (148.44) <sup>a</sup>	74.19 (0.02) <sup>a</sup>
M3	51.74 (3.5) <sup>b</sup>	4991.92 (117.05) <sup>b</sup>	69.14 (1.78) <sup>b</sup>
M4	48.59 (3.5) <sup>b</sup>	4401.69 (206.57) <sup>c</sup>	67.85 (0.72) <sup>b</sup>

Common corresponding letters (a-c) in a given column indicate no significant difference.

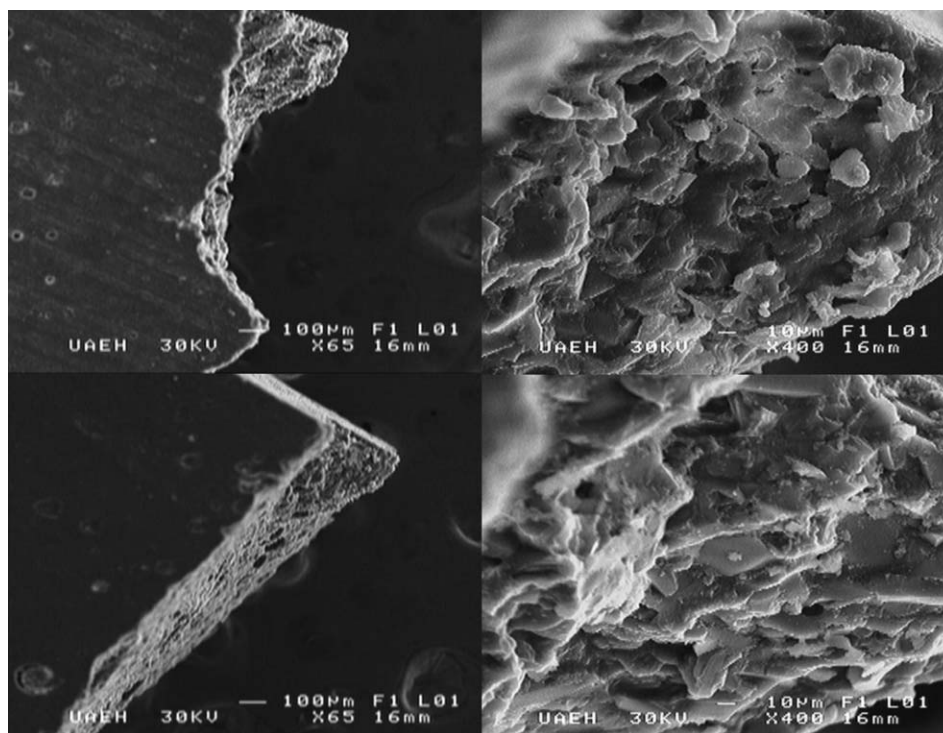


**Figure 7.** SEM images of the fracture surfaces of resin composites.

monomers. The concentration of double bonds in the dental composite resins is reduced with the increase of the molecular weight of the monomer, and therefore, the composite formulated with the MB-Phe-OH achieved higher values of double bond conversion. Also, the increased double bond conversion in the composite, produce highly crosslinked polymer and lower amount of residual monomer in the polymer network. This is desirable, because the residual monomer trapped in the composite may reduce its biocompatibility and clinical serviceability. Oxidation and hydrolytic degradation of the monomer may occur and involve some discoloration or accelerated wear.<sup>2–41</sup>

### Flexural Properties

In terms of flexural properties, the composite resin which contains MB-Phe-OH as diluent statistically presented significantly higher differences compared with the rest of the materials. Also, MB-Cis-OH and MB-1,7-OH composites did not present significant differences compared with BisGMA control. The composite with the MB-1,7-OH monomer had the rather than flexural modules.

According to Sideridou et al., the flexural test is the most appropriate measure of the strength because a material could only fail by the separation of the planes of atoms or by the slipping of the planes of atoms.<sup>42</sup> Clinically, dental composite resins are subjected to complex mastication forces with a considerable amount of flexural stress, and thus, restorations are subjected to large masticatory stresses where a high flexural strength is desired. The minimum requirement specified in ISO 4049 for the flexural strength is above 50 MPa. All materials except the MB-1,7-OH composite fulfill this requirement. The dental

composite resins with MB-Phe-OH showed the best performance regarding flexural properties. This could be correlated with the double bond conversion in which this composite showed higher values. It is well established that the double bond conversion affects the properties of the composite. Some authors state that higher double bond conversion improves final mechanical properties.<sup>20,43–47</sup> On the other hand, the presence of a rigid aromatic structure in the center of the MB-Phe-OH monomer leads to a better mechanical performance because such rings in the organic polymer of this composite resin allow the formation of noncovalent pi-pi stacking interaction. This molecular arrangement reinforces the macroscopic properties of the polymeric network, and therefore improves the final mechanical properties of the composite resins.<sup>30,48</sup> Some monomers described in the literature show similar behavior. He et al. synthesized a new trimethacrylate monomer with higher flexural strength than Bis-GMA-based resins, the enhanced properties were attributed to the phenyl groups in the monomer.<sup>49</sup> Pereira et al.<sup>47</sup> reported the synthesis of two Bis-GMA analogues with increased degree of conversion, due the higher flexibility of the less viscous monomers. Also, the monomers synthesized by Kilambi et al.<sup>50</sup> which were used as comonomers in Bis-GMA based resins obtaining dental composites with higher flexural modulus.

Only the composite formulated with the MB-1,7-OH monomer showed less flexural modules than Bis-GMA control. This confirms the previous reports where bis methacrylates with aliphatic groups produce flexible polymers.<sup>51</sup> Also, if the monomer is very flexible and not sufficiently bulky, mechanical properties will be poor.<sup>52</sup> MB-1,7-OH composite exhibits this



feature because of its structure where long hydrocarbon chain can be found. This gives it the ability to act as a plasticizer reducing the elastic modulus of the final material. This result agrees with Podgorski, who previously reported that the increase of the distance between double bonds decreases flexural modulus and hardness.<sup>32</sup>

Fracture surfaces of dental resins composites evaluated in this study were characterized by scanning electron microscopy. Figure 7 shows the fracture surface, silicon dioxide particles were randomly distributed in the composites and no appreciable resin-to-filler gaps appeared. This could confirm adequate silanization of the inorganic filler. Small voids are present because of nanoparticles nature, due their high specific area, they tend to aggregate in small agglomerates, so it is very difficult to disperse them homogeneously in the hydrophobic matrix. These characteristics were observed in all specimens evaluated. According to these images, the mechanical behavior of composites prepared is mainly influenced by organic matrix composition.

## CONCLUSIONS

The dental composite materials with MB-Cis-OH and MB-1,7-OH monomers showed double bond conversion and flexural properties comparable to those exhibited by the Bis-GMA/TEGDMA dental composite used as the control in this study. Materials with the MB-Phe-OH monomer showed higher double bond conversion and flexural properties compared with the dental resin control. The higher double bond conversion and the mechanical properties of the composite materials with MB-Phe-OH were attributed to their molecular structure, crosslinking capability, and molecular weight of the monomer. These results proved that MB-Phe-OH has the capability to be used as an ingredient in contemporary dental resin monomer systems with improved mechanical properties.

## ACKNOWLEDGMENTS

The authors acknowledge the Bilateral Cooperation Program MINCYT-CONACYT projects MX/09/04-J010.195 and CB-00168071.

## REFERENCES

1. Moszner, N.; Salz, U., *Prog. Polym. Sci.* **2001**, *26*, 535.
2. Anseth, K. S.; Goodner, M. D.; Reil, M. A.; Kannurpatti, A. R.; Newman, S. M.; Bowman, C. N. *J. Dent. Res.* **1996**, *75*, 1607.
3. Ferracane, J. L. *Dent. Mater.* **2011**, *27*, 29.
4. Peutzfeldt, A. *Eur. J. Oral Sci.* **1997**, *105*, 97.
5. Hervas-Garcia, A.; Martinez-Lozano, M. A.; Cabanes-Vila, J.; Barjau-Escribano, A.; Fos-Galve, P. *Med. Oral Patol. Oral Cir. Bucal.* **2006**, *11*, E215.
6. Vasudeva, G. *J. Calif. Dent. Assoc.* **2009**, *37*, 389.
7. Zimmerli, B.; Strub, M.; Jeger, F.; Stadler, O.; Lussi, A. *Schweiz Monatschr Zahnmed* **2010**, *120*, 972.
8. Tsai, M.-H.; Lin, Y.-K.; Chang, C.-J.; Chiang, P.-C.; Yeh, J.-M.; Chiu, W.-M.; Huang, S.-L.; Ni, S.-C. *Thin Solid Films* **2009**, *517*, 5333.
9. Tsai, M.-H.; Chang, C.-J.; Chen, P.-J.; Ko, C.-J. *Thin Solid Films* **2008**, *516*, 5654.
10. Chang, C.-J.; Tzeng, H.-Y. *Polymer* **2006**, *47*, 8536.
11. Braga, S. R.; Vasconcelos, B. T.; Macedo, M. R.; Martins, V. R.; Sobral, M. A. *Quintessence Int.* **2007**, *38*, e189.
12. Burke, F. J.; Cheung, S. W.; Mjor, I. A.; Wilson, N. H. *Quintessence Int.* **1999**, *30*, 234.
13. Deligeorgi, V.; Mjor, I. A.; Wilson, N. H. *Prim Dent Care* **2001**, *8*, 5.
14. Frost, P. M. *Prim Dent Care* **2002**, *9*, 31.
15. Mjor, I. A.; Moorhead, J. E.; Dahl, J. E. *Int. Dent. J.* **2000**, *50*, 361.
16. Tyas, M. J. *Aust. Dent. J.* **2005**, *50*, 81.
17. Jandt, K. D.; Sigusch, B. W. *Dent. Mater.* **2009**, *25*, 1001.
18. Chung, K. H.; Greener, E. H. *J. Oral Rehabil.* **1990**, *17*, 487.
19. Lopez-Suevos, F.; Dickens, S. H. *Dent. Mater.* **2008**, *24*, 778.
20. Palin, W. M.; Fleming, G. J.; Burke, F. J.; Marquis, P. M.; Randall, R. C. *J. Dent.* **2003**, *31*, 341.
21. Souza, R. O.; Ozcan, M.; Michida, S. M.; de Melo, R. M.; Pavanelli, C. A.; Bottino, M. A.; Soares, L. E.; Martin, A. A. *J. Prosthodont.* **2010**, *19*, 218.
22. Chen, T. M.; Brauer, G. M. *J. Dent. Res.* **1982**, *61*, 1439.
23. Wilson, K. S.; Zhang, K.; Antonucci, J. M. *Biomaterials* **2005**, *26*, 5095.
24. Vogel, A. I.; Furniss, B. S. *Vogel's Textbook of Practical Organic Chemistry*; Longman: London, **1989**.
25. Kim, J. W.; Kim, L. U.; Kim, C. K.; Cho, B. H.; Kim, O. Y. *Biomacromolecules* **2006**, *7*, 154.
26. Liu, F.; He, J. W.; Lin, Z. M.; Ling, J. Q.; Jia, D. M. *Molecules* **2006**, *11*, 953.
27. He, J.; Liao, L.; Liu, F.; Luo, Y.; Jia, D. *J. Mater. Sci. Mater. Med.* **2010**, *21*, 1135.
28. He, J.; Luo, Y.; Liu, F.; Jia, D. *J. Biomater. Sci. Polym. Ed.* **2010**, *21*, 1191.
29. Kurata, S.; Yamazaki, N. *Dent. Mater. J.* **2011**, *30*, 103.
30. Odian, G. G. *Principles of Polymerization*; Wiley-Interscience: Hoboken, NJ, **2004**.
31. He, J.; Liu, F.; Luo, Y.; Jia, D. *J. Appl. Polym. Sci.* **2012**, *125*, 114.
32. Podgorski, M. *Dent. Mater.* **2010**, *26*, e188.
33. Buruiana, E. C.; Jitaru, F.; Melinte, V.; Buruiana, T. *J. Appl. Polym. Sci.* **2013**, *127*, 2442.
34. Kaas, R. L.; Kardos, J. L. *Polym. Eng. Sci.* **1971**, *11*, 11.
35. Antonucci, J. M.; Dickens, S. H.; Fowler, B. O.; Xu, H. H. K.; McDonough, W. G. *J. Res. Natl. Inst. Stand. Technol.* **2005**, *110*, 541.
36. Debnath, S.; Wunder, S. L.; McCool, J. I.; Baran, G. R. *Dent. Mater.* **2003**, *19*, 441.
37. Mohsen, N. M.; Craig, R. G. *J. Oral Rehabil.* **1995**, *22*, 183.
38. Liu, Q.; Ding, J.; Chambers, D. E.; Debnath, S.; Wunder, S. L.; Baran, G. R. *J. Biomed. Mater. Res.* **2001**, *57*, 384.



39. Karabela, M. M.; Sideridou, I. D. *Dent. Mater.* **2011**, *27*, 825.
40. Fouassier, J. P.; Rabek, J. F. *Radiation Curing in Polymer Science and Technology*; Springer: London, **1993**.
41. Tanaka, K.; Taira, M.; Shintani, H.; Wakasa, K.; Yamaki, M. *J. Oral Rehabil.* **1991**, *18*, 353.
42. Sideridou, I. D.; Karabela, M. M.; Bikiaris, D. N. *Dent. Mater.* **2007**, *23*, 1142.
43. Lovell, L. G.; Lu, H.; Elliott, J. E.; Stansbury, J. W.; Bowman, C. N. *Dent. Mater.* **2001**, *17*, 504.
44. Ferracane, J. L.; Greener, E. H. *J. Biomed. Mater. Res.* **1986**, *20*, 121.
45. Santini, A.; Miletic, V.; Swift, M. D.; Bradley, M. J. *Dent.* **2012**, *40*, 577.
46. Lovell, L. G.; Newman, S. M.; Donaldson, M. M.; Bowman, C. N. *Dent. Mater.* **2003**, *19*, 458.
47. Pereira, S. G.; Osorio, R.; Toledano, M.; Nunes, T. G. *Dent. Mater.* **2005**, *21*, 823.
48. Seymour, R. B.; Carraher, C. E. *Introducción a la química de los polímeros*; Reverté, **1995**.
49. He, J.; Luo, Y.; Liu, F.; Jia, D. *J. Biomater. Appl.* **2010**, *25*, 235.
50. Kilambi, H.; Cramer, N. B.; Schneidewind, L. H.; Shah, P.; Stansbury, J. W.; Bowman, C. N. *Dent. Mater.* **2009**, *25*, 33.
51. Khatri, C. A.; Stansbury, J. W.; Schultheisz, C. R.; Antonucci, J. M. *Dent. Mater.* **2003**, *19*, 584.
52. Shobha, H. K.; Sankarapandian, M.; Kalachandra, S.; Taylor, D. F.; McGrath, J. E. *J. Mater. Sci. Mater. Med.* **1997**, *8*, 385.